On the Nature of the Solar Chromosphere

Robert J. Rutten

Sterrekundig Instituut, Utrecht University, The Netherlands
Institute of Theoretical Astrophysics, University of Oslo, Norway

Abstract.   DOT high-resolution imagery suggests that only internetwork-spanning Hα "mottles" constitute the quiet-Sun chromosphere, whereas more upright network "straws" in "hedge rows" reflect transition-region conditions.

1.   Introduction

In my talk I skipped a planned discourse on definitions of the chromosphere because Philip Judge had just admirably done so (these proceedings). I then used movies from the Dutch Open Telescope[1] (Rutten et al. 2004) to argue that much so-called chromosphere is actually transition region, that much other so-called chromosphere is actually upper photosphere, and that only those Hα mottles and fibrils that span across and between internetwork cells and active regions constitute the actual chromosphere. I compress the argument here into a two-figure summary of the evidence and a list of brief conjectures with explanatory cartoons. The upshot is that radiation modeling of the field-guided filamentary features (mottles, fibrils, spicules, "straws") that infest – if not constitute – the quiet-Sun domain between photosphere and corona should mix steep gradients in varied configurations with thick-to-thin radiation simulation, containing everything from LTE to coronal conditions. One conjecture is that the latter dominate such things as Ca II H & K superbasal magnetic-activity emissivity, making that a transition-region diagnostic.

2.   Evidence

Figure 1 shows Ca II H "straws" at right: long thin emission features in Ca II H, in rows jutting out from active network, seen near the limb against a dark background of reversed granulation. The latter is photospheric and is sampled only slightly deeper in the other two images.

   Figure 2 shows active network on the disk. The strikingly bright Hα-wing network bright points form in the deep photosphere; the different-morphology Ca II H network bright points form higher up. The Hα core shows its proprietary filamentary structures habitually called "mottles" in quiet Sun, "fibrils" when jutting out from active regions, "spicules" off the limb. Those in Figure 2 are

---

[1]All DOT data are public and available at the DOT database `http://dot.astro.uu.nl`. The movies that I showed and sample here in Figures 1 and 2 reside there also, under *DOT movies.*
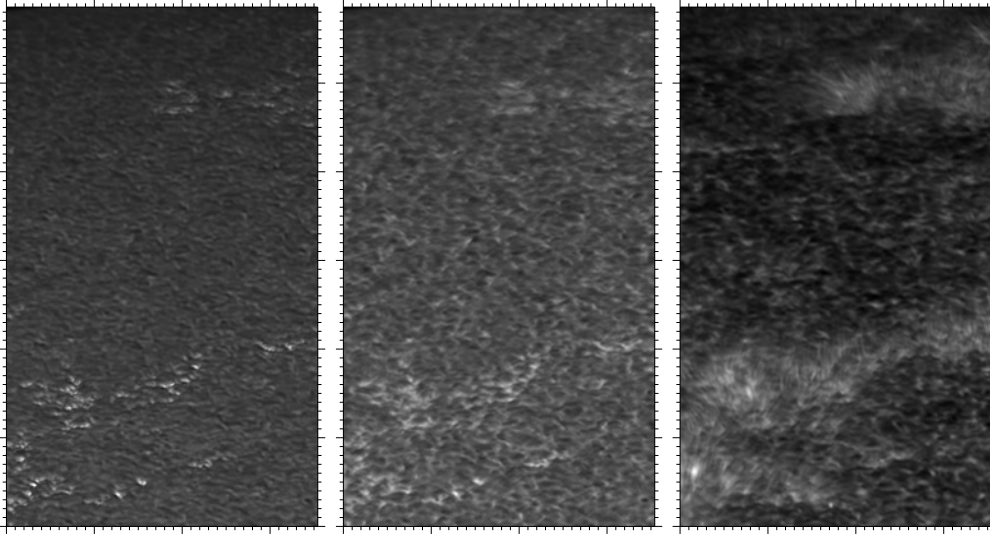
Figure 1.   Three partial near-limb images taken on June 18, 2003. Ticks at arcsecond intervals. The limb is just above the top. The first two are simultaneous, the third was taken 25 seconds earlier. *Left*: G band, showing the onset of reversed granulation and short bright stalks where our view penetrates through relatively empty network fluxtubes into hot granules. *Center*: Ca II H wing, a similar scene sampled slightly higher up. *Right*: Ca II H line center. The dark background consists of reversed granulation sampled by the inner-wing contributions within the 1.4 Å FWHM passband wherever the Ca II H core contributes insignificant magnetic-feature emission. Some internetwork features may mark acoustic shocks (but H_{2V} "grain" amplification from H_3 blueshift may lack along these slanted lines of sight). The active network is characterized by crowded forests of long thin bright features contributed by the line core. They are obviously optically thin. They are mostly upright since the internetwork foreground remains dark out to their bottoms. They start close to the photospheric network bright points. They are very dynamic (`http://dot.astro.uu.nl/movies/2003-06-18-mu034-ca-core.mpg`). I call them "straws" but my Utrecht colleagues prefer "grass".

mottles but with large-scale organization from avoiding the filament (the campaign target) just outside these cutouts. They tend to have bright near-network beginnings, especially in active plage.

The Hα disk mottles are not seen in Ca II H. Reversely, Ca II H limb straws do not stand out between all other mottles seen in Hα line center near the limb. They gain hedge-row prominence there only in the outer Hα wings, as slender isolated dark features against the bright Hα-wing background which appears when the internetwork is no longer occulted by cell-spanning mottles.

The VAULT-2 Lyα images at `http://wwwsolar.nrl.navy.mil/rockets/vault/archives.html` (*cf.* Korendyke et al. 2001) show dense, 5000 km-high hedge rows of abruptly ending bright upright straws above network near the limb, twice as high and much thicker than in Ca II H. In addition, they show weaker and flatter rosettes fanning out from network that also end abruptly, an
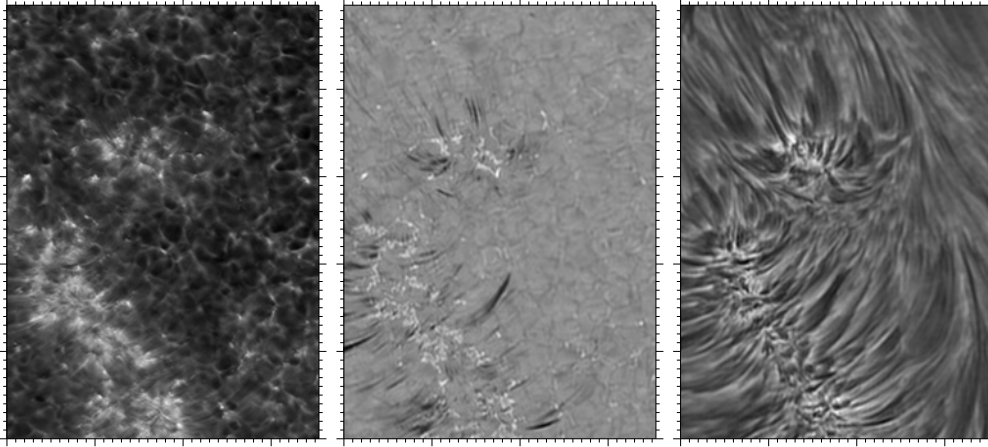
Figure 2.   Three partial disk-center images taken simultaneously on October 6, 2004.   Ticks at arcsecond intervals.   A filament lay along the righthand side of this cutout (`http://dot.astro.uu.nl/movies/` `2004-10-06-filament-4p.mpg`). *Left*: Ca II H. The internetwork shows reversed granulation contributed by the inner wings, superimposed acoustic H_{2V} grains, and a few isolated magnetic elements ("persistent flashers"). The network bright points are less sharp then and differ in morphology from G-band bright points. Bright stalks emanate a few arcseconds from them at this resolution (visible at high resolution). Diffuse Ca II H core brightness spreads as far or further. *Center*: blue Hα wing at 800 mÅ from line center. The internetwork consists of normal granulation at very low contrast. Photospheric magnetic elements appear very bright for various reasons explained by Leenaarts et al. (2005). Their morphology is identical to G-band bright points although they are less sharp at given telescope resolution. The very dark streaks that emanate from the network, often starting at some distance, frequently appear so dark through blueshift. Their abrupt outer ends vary rapidly in location. *Right:* Hα line center. A mass of extended mottles. They curve away from the neutral line under the filament. They appear intransparent. Their frequently bright beginnings are near to, but not co-spatial with, yet brighter network grains that have a closer resemblance to the Ca II H ones than to the Hα -wing ones.

opaque dark floor of long mottles covering internetwork areas. On-disk plage appears as a dense forest of short bright stalks and bright grains.

Comparison of the Ca II H, Hα and Lyα scenes raises questions:

1. Similarities: how can these various structures appear simultaneously in Lyα, Hα, and Ca II H? A similar question to the old one of why off-limb spicules appear in all of He I D$_3$, Hα, and Ca II K, but adding Lyα.

2. Differences: the hedge rows of upright straws are bright and optically thick in Lyα, bright and thin in Ca II H, much less distinct and dark in the Hα line center, more prominent but less upright and very dark in the Hα wings. The cell-spanning Hα mottles are not seen in Ca II H and only as a dark floor in Hα. Why?

3. Considerations

The left part of Figure 3 is a schematic consideration of the scenes in Figure 1. Mid-photosphere regime A (tenuous fluxtubes in reversed granulation) is currently well understood: time-dependent magnetoconvection plus LTE radiation simulations explain G-band bright points and reversed granulation very well (Shelyag et al. 2004, Keller et al. 2004, Carlsson et al. 2004, Leenaarts & Wedemeyer-Böhm 2005). Internetwork upper-photosphere regime B requires time-dependent NLTE modeling as in the acoustic shock simulation of Carlsson & Stein (1997), but does not produce noticeable Ca II H emission outside acoustic grains because the shocks do not heat on average. Internetwork regime C is transparent in Ca II H. Fluxtube regime E makes the straws in Figure 1 bright. Fluxtube regime F starts where they end, corresponding to spicule heights on the limb.

Since the straws appear without contributions from regimes B and C their intensity is, in homogeneous-cloud approximation:

$$I \approx B(T_{\mathrm{A}}) \, \mathrm{e}^{-\tau_{\mathrm{s}}} + S_{\mathrm{s}} \left[1 - \mathrm{e}^{-\tau_{\mathrm{s}}}\right] \approx B(T_{\mathrm{A}}) + [S_{\mathrm{s}} - B(T_{\mathrm{A}})] \, \tau_{\mathrm{s}}, \qquad (1)$$

where T_{A} is the $\tau = 1$ background temperature and τ_{s} the optical thickness of the straw along the line of sight. The second version requires $\tau_{\mathrm{s}} \ll 1$. The straw source function is:

$$S_{\mathrm{s}} = \left[(1 - \varepsilon) \, \overline{J} + \varepsilon \, B(T_{\mathrm{s}}) + \eta \, B^{*}\right] / (1 + \varepsilon + \eta) \approx (b_u/b_l) \, B(T_{\mathrm{s}}), \qquad (2)$$

adding the contributions from resonant scattering, thermal lower-to-upper level excitation, and multi-level roundabout photon production. In the optically thin limit without irradiation (as in coronal conditions) use of the emissivity and geometrical straw thickness D is more direct: $I \approx S_{\mathrm{s}} \, \tau_{\mathrm{s}} = j_{\mathrm{s}} \, D = (h\nu/4\pi) \, n_u \, A_{ul} \, D$.

4. Conjectures

1. Structures: there are four distinct types of filamentary structures in the quiet-Sun regime between photosphere and corona, sketched at right in Figure 3. Type 1 and 2 connect upward into hot conditions where they end abruptly. Type 1 is rather straight and upright, remains slender to large height, and is hot and dense from unidentified mass and energy filling. Type 2, often arranged in sheets, is less hot from propagative p-mode mass loading from below as suggested by De Pontieu et al. Type 3 is supposedly loaded similarly or by siphoning, but does not connect into hot conditions and remains cool. Type 4 is conjectured by Schrijver & Title (2003) but is hard to observe if neither evacuation nor filling gives them brightness signature.

2. Regimes: the regime C surroundings of types 1–3 are transparent in Ca II H, H α, and Ly α, most likely from being coronally hot and tenuous. Upper-photosphere regime B is cool outside shocks, does not produce much Ca II H line-center emissivity, is transparent throughout H α due to low H I $n = 2$ population, and is largely shielded by type-3 loops in Ly α and H α center.
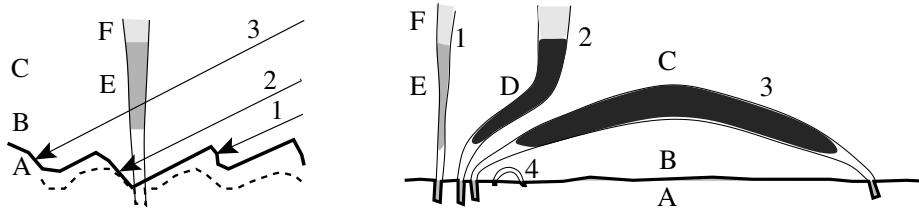
Figure 3. *Left*: near-limb Ca II H observation. Line of sight 1 hits $\tau = 1$ (thick curve along the bottom, the dashed curve is $\tau = 1$ for radial viewing) in a granule and produces low brightness $I \approx B(\tau = 1)$ in the inner wings of Ca II H which sample reversed granulation in the middle photosphere (regime A). It passes first through internetwork regime C which is fully transparent in Ca II H. The contribution of line-center emission by acoustic shocks in upper-photosphere regime B is also small. Line 2 hits another granule after passing through a fluxtube that is relatively empty at low height. The smaller opacity buildup results in deeper sampling than along lines parallel to line 2 in the plane perpendicular to the sketch but missing the fluxtube similarly to line 1. The granular interior therefore appears as a short bright stalk in the Ca II H wings. Line of sight 3 also hits a granule after passing through the fluxtube, but higher up through regime E which contributes the straw brightness.
Right: different filamentary structures. A similar cartoon is shown in Figure 2 of Fontenla et al. (1993); compare also Judge's sketch in these proceedings. Rough temperatures: $D \sim 10^4$ K, $E \sim 10^5$ K, $F \sim 10^6$ K. Outside regimes: A = photosphere with normal/reversed granulation and tenuous magnetic elements, B = upper internetwork photosphere pervaded by acoustic shocks but nevertheless cool, C = transparent in H & K, H α, and Ly α. *Type 1*: bright upright H & K and Ly α network straws opening into coronal plasma. On the disk they produce grainy H & K line-center, H α line-center, and Ly α full-profile emission in network and plage (Figure 2). *Type 2*: dark H α mottles bending upward into hot plasma from unipolar crowding. They represent the on-disk "spicules" modeled by De Pontieu et al. (2004) as due to p-mode mass loading. They end abruptly where the shocked cool gas meets transition-region temperatures. Above plage they cause rapid occultive flickering of TRACE 171 Å brightness ("moss") through bound-free hydrogen and helium scattering out of the TRACE passband (Berger et al. 1999, Rutten 1999). *Type 3*: dark H α mottles spanning across cell interiors in bipolar network without hot-plasma connectivity. They are reasonably well represented by the classical modeling of Giovanelli (1967), Beckers (1968, 1972), Heinzel & Schmieder (1994) as opaque clouds of order 10^4 K. *Type 4*: short weak-field near-network loops postulated by Schrijver & Title (2003). They lack the Wilson depressions that turns types $1-3$ into bright points in photospheric diagnostics and the mass loading that makes types 2 and 3 dark in chromospheric H α.

3. Ly α: type 1 produces the thick hedge rows of network straws in the VAULT-2 near-limb images. Their appearance suggests thermal Ly α emission from optically thick straws with $I \approx S_s \approx \varepsilon_s B(T_s)$ if effectively thin and growing to $\sqrt{\varepsilon_s}\, B(T_s)$ for the thickest ones. Since ε is likely small, T_s must be high. The bright grains abounding in disk plage are due to type-1 along-the-straw viewing. The abruptly ending rosette fans correspond to type 2. Type 3 constitutes the dark opaque internetwork background, with $I \approx \sqrt{\varepsilon_3}\, B(T_3)$. Regime C must be transparent through being coronal, not only hot but

also tenuous since at coronal temperatures H I maintains as much as 10^{-6} fractional population (J. Raymond).

4. Other UV lines: type 1 produces network brightness in UV lines across many stages of ionization. The systematic downdrafts observed in these suggest energy transfer from above.

5. Ca II H: type 1 also produces the Ca II near-limb straws, in similar fashion to the Ly α ones but at smaller opacity, half as long, and with photospheric internetwork background. The $\eta B^\star$ contribution in Equation (2) is likely important through dielectronic recombination since Ca II ionizes to closed-shell Ar configuration. It still has 10^{-3} fractional population at $T = 10^5$ K in coronal conditions (Mazzotta et al. 1998), or nearly 1% of the H I $n=2$ population density. In any case, Ca II level $n=2$ must have considerable population in the straws compared to regime C. Somewhere along the flux-tube the magnetic-element brightness must flip from being due to evacuation to being due to excess filling (*cf.* Sheminova et al. 2005). On the disk, viewing along straws produces the bright Ca II H network grains and the short bright filaments jutting out from the Ca II H network at high resolution (Figure 2). The straws also cause the wide-spread diffuse Ca II H brightness around network, the diffuseness arising from lack of resolution, small optical thickness through slanted straws, and resonance and electron scattering.

6. H α on the disk: type-3 mottles occult the underlying photosphere at line center. They can be dark or bright (*cf.* Heinzel & Schmieder 1994), especially when images are scaled for optimum display contrast. Type 2 produces dark mottles jutting out from network with abrupt endings. Following the conjecture by De Pontieu et al. they should show substantial five-minute modulation in their Dopplershift and endpoint locations. The bright beginnings of type 2 and 3 mottles that are frequently observed near active network and plage are likely due to $S \approx \eta B^\star$ Lyman (lines and continuum) irradiation by type-1 straws. Type 1 appears also in on-the-disk H α line center as bright grains and diffuse emission. In the wings only type-2 structures remain visible, always dark because the photospheric background $B(T_A)$ is relatively bright in H α (Leenaarts et al. 2005). Dopplershifts cause extra type-2 darkening, most frequently in the blue wing through blueshift.

7. H α at the limb: types 1 and 2 gain H α conspicuousness in the line wings in which type 3 vanishes. Larger line width increases their far-wing visibility on the disk but decreases their off-limb contrast as spicules (A. G. de Wijn).

8. Modeling: chromospheric modeling should upgrade to the comprehensive VAL/FAL radiation treatment of Vernazza et al. (1981) and Fontenla et al. (1993) which covers the whole gamut from high-density LTE in their photospheric bottoms through NLTE and PRD to coronal conditions at their $T = 10^5$ K model tops – but not in 1D radial geometry but for chromospheric cylinders and sheets, with variation in orientation, density, and temperature, embedded in coronal or upper-photosphere surroundings, and possessing transition-region sheaths to these and upward coronal contact as

in types 1 and 2. The next step is to feed them mass from below through dynamic pistoning including p-modes and convective squirting (Babcock & Babcock 1955), and energy from above through conduction.

9. Nomenclature: the *chromosphere* consists primarily of type-3 mottles and fibrils. They appear as a crowded Hα forest at the limb and collectively cause the purple Hα + Hβ flash at the onset of totality for which the chromosphere is rightfully named. Later definitions as "initial outward temperature rise" or "layer between the temperature minimum and the transition region" should be disavowed. Regime B, extending over $h \approx 400-1300$ km, is non-purple "upper photosphere" or "clapotisphere" (Rutten 1995). Regime C is coronal. The *transition region* is extremely warped, consisting of the regime E parts of type-1 straws plus the D-F interface in type 2 mottles plus thin low-emissivity D-F sheaths along type 2 and 3 mottles. As a spherical shell it exists only around the fictitious but superbly didactic star VALIII (Rutten 2003).

10. Cool-star activity: the superbasal "Ca II emission" which is so useful as stellar activity indicator (Rutten et al. 1991, Schrijver 1995) comes primarily from type 1 structures, just like Lyα and other UV lines. That's why Ca II H & K excess flux correlates so well with UV line fluxes. H & K network bright points are "transition region" diagnostics just like those.

References

Babcock, H. W. & Babcock, H. D., 1955, ApJ 121, 349

Beckers, J. M., 1968, Solar Phys. 3, 367

Beckers, J. M., 1972, ARA&A 10, 73

Berger, T. E., De Pontieu, B., Fletcher, L., Schrijver, C. J., Tarbell T. D., & Title, A. M., 1999, Solar Phys. 190, 409

Carlsson, M. & Stein, R. F., 1997, ApJ 481, 500

Carlsson, M., Stein, R. F., Nordlund, Å., & Scharmer, G. B., 2004, ApJ 610, L137

De Pontieu, B., Erdélyi, R., & James, S. P., 2004, Nat 430, 536

Fontenla, J. M., Avrett, E. H., & Loeser, R., 1993, ApJ 406, 319

Giovanelli, R. G., 1967, Austr. J. Phy. 20, 81

Heinzel, P. & Schmieder, B., 1994, A&A 282, 939

Judge, P. 2006, in ASP Conf. Ser. Vol. 354, Solar MHD: Theory and Observations – a High Spatial Resolution Perspective, ed. H. Uitenbroek, J. Leibacher, & R. Stein (San Francisco: ASP), 259

Keller, C. U., Schüssler, M., Vögler, A., & Zakharov, V., 2004, ApJ 607, L59

Korendyke, C. M., Vourlidas, A., Cook, J. W., Dere, K. P., Howard, R. A., Morrill, J. S., Moses, J. D., Moulton, N. E., & Socker, D. G., 2001, Solar Phys. 200, 63

Leenaarts, J., Rutten, R. J., Sütterlin, P., Carlsson, M., & Uitenbroek, H., 2006, A&A 449, 1209

Leenaarts, J. & Wedemeyer-Böhm, S., 2005, A&A 431, 687

Mazzotta, P., Mazzitelli, G., Colafrancesco, S., & Vittorio, N., 1998, A&AS 133, 403

Rutten, R. G. M., Schrijver, C. J., Lemmens, A. F. P., & Zwaan, C., 1991, A&A 252, 203

Rutten, R. J., 1995, in ESA SP-376, Proc. 4th SOHO Workshop, Helioseismology, ed. J. T. Hoeksema, V. Domingo, B. Fleck, & B. Battrick (Noordwijk: ESA), 151

Rutten, R. J., 1999, in ASP Conf. Ser. Vol. 184: Third Advances in Solar Physics Euroconference: Magnetic Fields and Oscillations, (San Francisco: ASP), p. 181

Rutten, R. J., 2003, Radiative Transfer in Stellar Atmospheres, Lecture Notes Utrecht University, 8th Edition, `http://www.astro.uu.nl/~rutten`

Rutten, R. J., Hammerschlag, R. H., Bettonvil, F. C. M., Sütterlin, P., & de Wijn, A. G., 2004, A&A 413, 1183

Schrijver, C., 1995, A&A Rev. 6, 181

Schrijver, C. J. & Title, A. M., 2003, ApJ 597, L165

Shelyag, S., Schüssler, M., Solanki, S. K., Berdyugina, S. V., & Vögler, A., 2004, A&A 427, 335

Sheminova, V. A., Rutten, R. J., & Rouppe van der Voort, L. H. M., 2005, A&A 437, 1069

Vernazza, J. E., Avrett, E. H., & Loeser, R., 1981, ApJS 45, 635